

Experimental and theoretical investigation of timing jitter inside a stretcher-compressor setup

Sandro Klingebiel,^{1,5,*} Izhar Ahmad,^{1,3,4,5} Christoph Wandt,¹
Christoph Skrobol,¹ Sergei A. Trushin,¹ Zsuzsanna Major,^{1,2}
Ferenc Krausz,^{1,2} and Stefan Karsch^{1,2}

¹Max-Planck-Institut für Quantenoptik, Hans-Kopfermann-Str. 1, D-85748 Garching, Germany

²Department für Physik, Ludwig-Maximilians-Universität München, Am Coulombwall 1, D-85748 Garching, Germany

³Optics Laboratories, PO 1021, Nilore, Islamabad, Pakistan

⁴izhar916@yahoo.com

⁵These authors contributed equally to this work

*sandro.klingebiel@mpq.mpg.de

Abstract: In an optically synchronized short-pulse optical-parametric chirped-pulse amplification (OPCPA) system, we observe a few-100 fs-scale timing jitter. With an active timing stabilization system slow fluctuations are removed and the timing jitter can be reduced to 100 fs standard deviation (Std). As the main source for the timing fluctuations we could identify air turbulence in the stretcher-compressor setup inside the chirped pulse amplification (CPA) pump chain. This observation is supported by theoretical investigation of group delay changes for angular deviations occurring between the parallel gratings of a compressor or stretcher, as they can be introduced by air turbulence.

© 2012 Optical Society of America

OCIS codes: (320.7120) Ultrafast phenomena; (320.5520) Pulse compression; (190.4970) Parametric oscillators and amplifiers; (140.3615) Lasers, ytterbium.

References and links

1. O. V. Chekhlov, J. L. Collier, I. N. Ross, P. K. Bates, M. Notley, C. Hernandez-Gomez, W. Shaikh, C. N. Dan-son, D. Neely, P. Matousek, S. Hancock, and L. Cardoso, "35 J broadband femtosecond optical parametric chirped pulse amplification system," *Opt. Lett.* **31**, 3665–3667 (2006).
2. V. V. Lozhkarev, G. I. Freidman, V. N. Ginzburg, E. V. Katin, E. A. Khazanov, A. V. Kirsanov, G. A. Luchinin, A. N. Malshakov, M. A. Martyanov, O. V. Palashov, A. K. Poteomkin, A. M. Sergeev, A. A. Shaykin, and I. V. Yakovlev, "Compact 0.56 petawatt laser system based on optical parametric chirped pulse amplification in KD*P crystals," *Laser Phys. Lett.* **4**, 421–427 (2007).
3. D. Herrmann, L. Veisz, R. Tautz, F. Tavella, K. Schmid, V. Pervak, and F. Krausz, "Generation of sub-three-cycle, 16 TW light pulses by using noncollinear optical parametric chirped-pulse amplification," *Opt. Lett.* **34**, 2459–2461 (2009).
4. P. Dietrich, F. Krausz, and P. B. Corkum, "Determining the absolute carrier phase of a few-cycle laser pulse," *Opt. Lett.* **25**, 16–18 (2000).
5. S. Karsch, Zs. Major, J. Fülöp, I. Ahmad, T. Wang, A. Henig, S. Kruber, R. Weingartner, M. Siebold, J. Hein, Chr. Wandt, S. Klingebiel, J. Osterhoff, R. Hörlein, and F. Krausz, "The petawatt field synthesizer: a new approach to ultrahigh field generation," in *Advanced Solid-State Photonics*, OSA Technical Digest Series (CD) (Optical Society of America, 2008), paper WF1.
6. Zs. Major, S. A. Trushin, I. Ahmad, M. Siebold, Chr. Wandt, S. Klingebiel, T.-J. Wang, J. A. Fülöp, A. Henig, S. Kruber, R. Weingartner, A. Popp, J. Osterhoff, R. Hörlein, J. Hein, V. Pervak, A. Apolonski, F. Krausz, and

- S. Karsch, "Basic concepts and current status of the petawatt field synthesizer—a new approach to ultrahigh field generation," *Rev. Laser Eng.* **37**, 431–436 (2009).
7. I. Ahmad, S. A. Trushin, Zs. Major, Chr. Wandt, S. Klingebiel, T.-J. Wang, V. Pervak, A. Popp, M. Siebold, F. Krausz, and S. Karsch, "Frontend light source for short-pulse pumped OPCPA system," *Appl. Phys. B* **97**, 529–536 (2009).
 8. D. Strickland and G. Mourou, "Compression of amplified chirped optical pulses," *Opt. Commun.* **55**, 447–449 (1985).
 9. S. Klingebiel, Chr. Wandt, C. Skrobol, I. Ahmad, S. A. Trushin, Zs. Major, F. Krausz, and S. Karsch, "High energy picosecond Yb:YAG CPA system at 10 Hz repetition rate for pumping optical parametric amplifiers," *Opt. Express* **19**, 5357–5363 (2011).
 10. N. Ishii, L. Turi, V. S. Yakovlev, T. Fuji, F. Krausz, A. Baltuska, R. Butkus, G. Veitas, V. Smilgevicius, R. Danielius, and A. Piskarskas, "Multimillijoule chirped parametric amplification of few-cycle pulses," *Opt. Lett.* **30**(5), 567–569 (2005).
 11. C. P. Hauri, P. Schlup, G. Arisholm, J. Biegert, and U. Keller, "Phase-preserving chirped-pulse optical parametric amplification to 17.3 fs directly from a Ti:sapphire oscillator," *Opt. Lett.* **29**(12), 1369–1371 (2004).
 12. D. Yoshitomi, X. Zhou, Y. Kobayashi, H. Takada, and K. Torizuka, "Long-term stable passive synchronization of 50 μ J femtosecond Yb-doped fiber chirped-pulse amplifier with a mode-locked Ti:sapphire laser," *Opt. Express* **18**, 26027–26036 (2010).
 13. C. Y. Teisset, N. Ishii, T. Fuji, T. Metzger, S. Köhler, R. Holzwarth, A. Baltuska, A. M. Zheltikov, and F. Krausz, "Soliton-based pump-seed synchronization for few-cycle OPCPA," *Opt. Express* **13**(17), 6550–6557 (2005).
 14. E. Treacy, "Optical pulse compression with diffraction gratings," *IEEE J. Quantum Electron.* **5**, 454–458 (1969).
 15. I. Ahmad, L. Berge, Zs. Major, F. Krausz, S. Karsch, and S. A. Trushin, "Redshift of few-cycle infrared pulses in the filamentation regime," *New J. Phys.* **13**, 093005 (2011).
 16. P. S. Banks, M. D. Perry, V. Yanovsky, S. N. Fochs, B. C. Stuart, and J. Zweiback, "Novel all-reflective stretcher for chirped-pulse amplification of ultrashort pulses," *IEEE J. Quantum Electron.* **36**, 268–274 (2000).
 17. T. Miura, K. Kobayashi, K. Takasago, Z. Zhang, K. Torizuka, and F. Kannari, "Timing jitter in a kilohertz regenerative amplifier of a femtosecond-pulse Ti:Al₂O₃ laser," *Opt. Lett.* **25**, 1795–1797 (2000).
 18. G. Pretzler, A. Kasper, and K. J. Witte, "Angular chirp and tilted light pulses in CPA lasers," *Appl. Phys. B* **70**, 1–9 (2000).
 19. O. E. Martinez, "3000 times grating compressor with positive group velocity dispersion: application to fiber compensation in 1.3 – 1.6 μ m region," *IEEE J. Quantum Electron.* **23**, 59–64 (1987).
 20. F. Adler, A. Sell, F. Sotier, R. Huber, and A. Leitenstorfer, "Attosecond relative timing jitter and 13 fs tunable pulses from a two-branch Er: fiber laser," *Opt. Lett.* **32**, 3504–3506 (2007).
 21. Q. Hao, W. Li, and H. Zeng, "High-power Yb-doped fiber amplification synchronized with a few-cycle Ti:sapphire laser," *Opt. Express* **17**, 5815–5821 (2009).

1. Introduction

State-of-the-art high-energy optical parametric chirped pulse amplification (OPCPA) systems are usually operated with stretched pulse durations in the range of 100 ps - ns (cf. Ref. [1–3]). In contrast to that the short-pulse OPCPA scheme uses much shorter pulses on the order of 1 ps. This significantly increases the pump power and permits the use of thinner OPA crystals while keeping the same level of gain, which implies an increase of amplification bandwidth as compared with OPA driven by longer pulses. Additionally the short pump-pulse duration reduces the necessary stretching factor for the broadband-seed pulse, thereby increasing stretching and compression fidelity and allowing the use of simple, high-throughput stretcher-compressor systems, consisting of bulk glass and chirped multilayer mirrors. Furthermore, the technique of few-ps OPCPA possesses immense potential for generating high contrast pulses due to the short, ps-scale time window for the parametric fluorescence. Nevertheless the high-energy pump laser is not commercially available and therefore needs to be developed.

The Petawatt Field Synthesizer (PFS) is based on the above introduced short-pulse OPCPA scheme. The PFS project aims at developing a petawatt-scale carrier-envelope phase [4] controlled light source to deliver pulses with energies of > 3 J in the few-cycle regime (< 5 fs, 700 – 1400 nm) at a repetition rate of 10 Hz [5–7]. The PFS design with several OPCPA stages requires a special, synchronized pump delivering 1 – 2 ps pulses with 4×5 J pulse energy (frequency doubled at 515 nm), i.e. 4×12 Joule in the fundamental beam (1030 nm) at 10 Hz repetition rate. The pump source with these specifications is based on the chirped-pulse ampli-

fication (CPA) principle [8] using Yb:YAG as the amplification medium pumped by high power laser diodes. At present, this source is capable of delivering 200 mJ pulses at 1030 nm with a compressed pulse duration of ≈ 1 ps [9].

Precise synchronization between pump and seed pulse is a prerequisite for stable amplification in the OPCPA stages, since the pulses are only 1 ps long. Simulations of the OPCPA amplification show, that 150fs timing jitter could result in significant spectral changes in the amplified signal, while the Fourier-limited pulse length changes only by 4%. Therefore we consider 150 fs as a tolerable upper limit for the timing jitter in a 1 ps OPCPA stage.

Different active, e.g Ref. [10], and passive optical synchronization schemes such as direct seeding [11], injection seeding [12] and frequency shifting using a photonic crystal fiber (PCF) [13] have already been developed, which allow for few-fs jitter between different amplifier chains. We apply the latter technique to derive both pump and seed pulses from the same oscillator. The initially synchronized pump beam has to be amplified prior to the OPCPA stage. In these amplifiers the pulse propagates along a significantly longer path than the seed pulses. This additional optical path amounts to several 100m in our case and makes the setup highly sensitive to mechanical vibrations and air fluctuations as sources of timing jitter. Therefore it is important to check the temporal synchronization at the position of the OPCPA stages.

In this paper we present the results of single-shot measurements of the relative timing between the pump and the seed pulses at 10 Hz repetition rate in order to quantify the level of synchronization in our experimental setup. Additionally we applied an active stabilization stage to reduce the jitter to 100 fs. We could identify air turbulence inside the stretcher-compressor setup of the CPA pump laser as the main source of the timing jitter by performing several measurements at different stages in the CPA pump laser chain. In order to investigate the influence of air fluctuations inside the stretcher/compressor on the timing of the pulse theoretically, we performed calculations for the optical path length with a small perturbation of the beam pointing inside a Treacy-type compressor [14].

2. Experimental setup

The schematic layout of our system is shown in Fig. 1. In order to achieve optical synchronization, both seed and pump pulses are derived from a common Ti:sapphire oscillator (*Rainbow, Femtolasers GmbH*), which serves as the master oscillator. For the generation of the OPCPA seed, a fraction of the oscillator output is amplified in a commercial Ti:sa amplifier (*Femtopower Compact-Pro, Femtolasers GmbH*) and subsequently compressed in a hybrid pulse compressor (HPC). The output of the HPC is used for generating a broadband supercontinuum by a two-stage spectral broadening technique. Details about the OPCPA seed generation are described in [7, 15]. The near-infrared spectral part (700 nm to 1400 nm) of this supercontinuum is then stretched to approximately 1 ps for seeding the first stage of the main OPCPA chain, which is under construction. For the OPCPA pump generation, a part of the oscillator output is spectrally shifted to 1030 nm in a PCF and amplified in a two-stage fiber amplifier to 1 W. In order to stretch the narrow bandwidth (ca. 4 nm) pulses to 3 ns we apply an all reflective stretcher [16] in a double-pass configuration (i.e. 8 reflections off the grating). After stretching, the amplification takes place in an Yb:glass regenerative amplifier (regen) followed by a multi-pass amplifier based on Yb:YAG, both of which are diode-pumped. The compression is realized with a Treacy-type compressor [14] with a large grating separation of 6 m, using the same gratings as in the stretcher (1740 lines/mm). After compression an energy of 200 mJ is delivered within 1 ps pulse duration. A more detailed description of the setup can be found in [9].

The path through the CPA pump chain would result in a total optical delay of $\approx 1 \mu\text{s}$ between the OPCPA pump and the seed at the position of the first OPCPA stage. In order to compensate

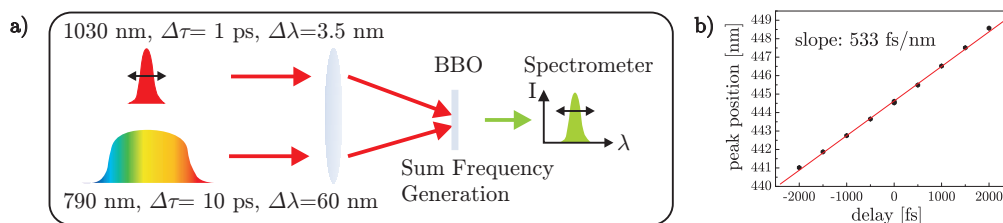


Fig. 2. a) Schematic picture of the modified cross-correlation technique [17]. The spectrum of the sum frequency signal between the short pump pulse and a long, chirped reference pulse is measured. The relative arrival time of the pulses is transformed into a frequency change of the sum frequency signal. b) Calibration curve for the used setup. The centroid of the sum frequency signal is measured at different relative delays.

between the pulses and measured the centroid of the spectrum. In Fig. 2(b) the calibration curve for the lowest jitter pulses (compare Fig. 3(b)) is shown. Each point is the mean value of 100 shots and the standard deviation is too small to resolve the error bars in the plot. For delays larger than 1 ps one can observe a deviation from the linear fit, which could be explained by higher order dispersion in the chirped pulse. In this delay range, a higher order fit would be more accurate. Nevertheless in the central part (± 1 ps), where we work, the linear fit is sufficiently accurate and no correction is needed. The calibration factor of 533 fs/nm of the linear fit is used for all of the following measurements.

4. Experimental results and discussion

Our findings are summarized in Fig. 3. The measured fluctuation of the relative timing between pump and seed are shown in Fig. 3(a). Here the pump pulse is stretched, fully amplified in the regenerative and multipass amplifiers and subsequently compressed. For this measurement no precautions were taken to reduce air fluctuations, i.e. the flowboxes were running. We find that the timing jitter has a standard deviation of 400 fs, which would be unacceptable for proceeding with the short-pulse pumped OPCPA experiments.

In order to determine the source of this measured rather large temporal oscillation, we studied the effect of the different components of the CPA pump-laser chain. First, we bypassed the stretcher-compressor setup and amplified the unstretched pulses (ca. 4 ps) in the regen to a low power level. The relative timing was then measured between the reference and the pulses amplified in the regen in case when i) the same pulses, and ii) different pulses with approximately 1 μ s delay (this delay is expected for the full amplifier chain including stretcher and compressor) were selected from the master oscillator for both chains. The appropriate optical delay is achieved by adjusting the number of round trips in the regen.

As depicted in Fig. 3(b), when the same pulses were selected for amplification in pump- and seed-chains (red curve), the jitter is hardly above the resolution of our measurement system. In the case with 1 μ s delay (black curve) one could expect different sources of jitter. On the one hand the repetition rate instability of the master oscillator introduces a jitter between the two selected pulses. Although the oscillator repetition rate is not stabilized, a low temporal jitter can be expected on a s timescale since the main causes for the change of the repetition rate, acoustic noise (1kHz-100Hz) and thermal fluctuations (1 Hz and below) act on a much slower timescale. On the other hand also the regen introduces optical delay fraught with jitter. Although both sources can not be distinguished by the described measurement, together they account for a few-10 femtosecond jitter. This is close to the resolution limit of our measurement setup, and is clearly well below our tolerable limit for the short-pulse pumped OPCPA. This

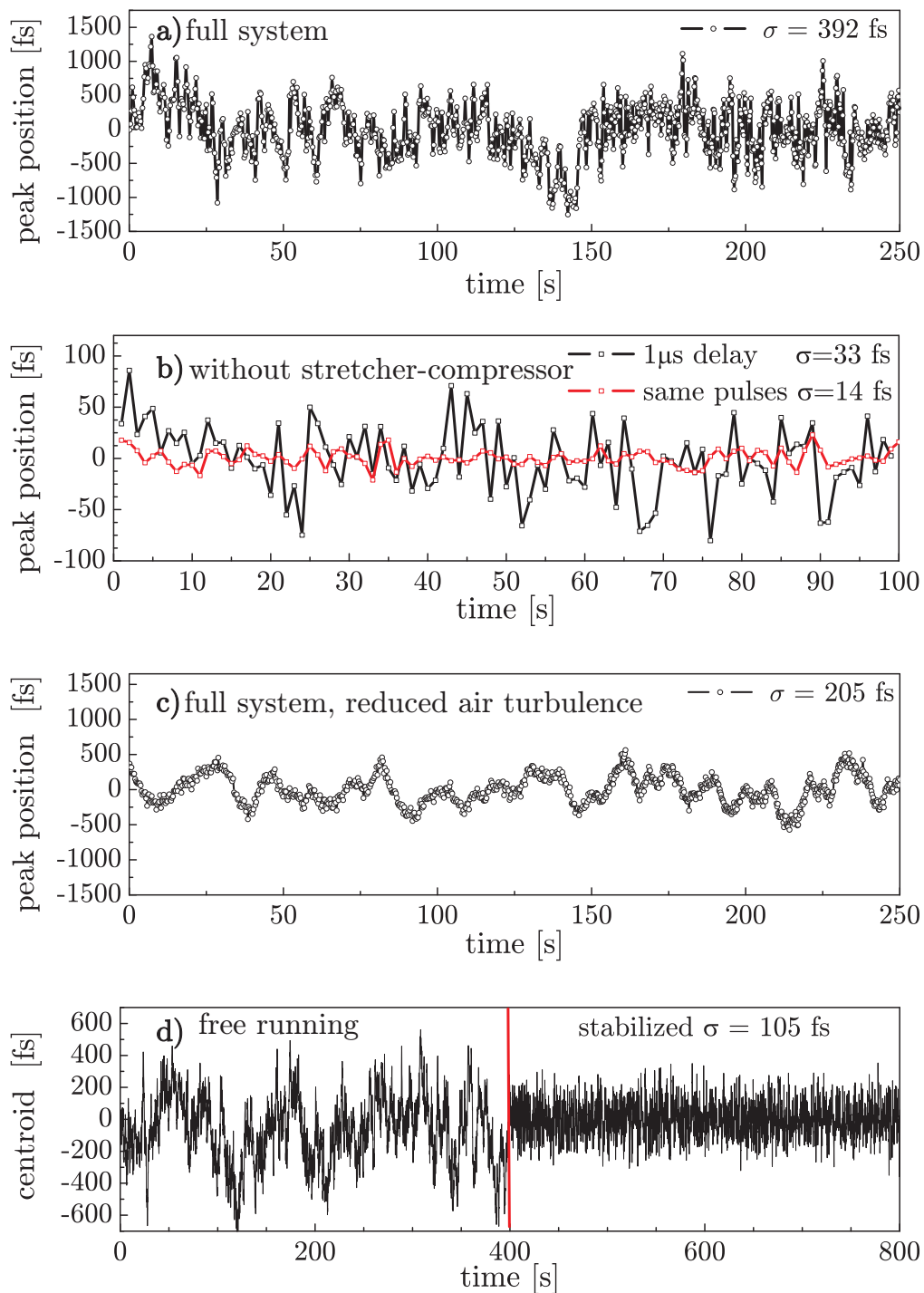


Fig. 3. Results of timing jitter measurements a) Pump pulse passes through the entire CPA chain: ± 400 fs timing jitter. b) Timing jitter when stretcher/compressor are bypassed: ± 14 fs when the same pulses are used from the master oscillator; ± 33 fs with $1\ \mu\text{s}$ delay. c) Pump pulse passes through entire CPA chain with precautions to reduce air turbulence: timing jitter consists of ± 70 fs shot-to-shot fluctuation and ± 200 fs slow oscillations. d) comparison between free running (left) and actively stabilized timing jitter (right).

means that the optical delay inside the regenerative amplifier has much less influence on the timing fluctuations compared to the same optical delay generated inside a stretcher-compressor setup. We can therefore conclude that the large timing oscillations, shown in Fig. 3(a) arise from the stretcher-compressor setup. We believe that the mechanical instabilities of different optomechanical components and air fluctuations along the long propagation distance contribute strongly to this timing instability. This argument is supported by Fig. 3(c), which shows again the pass through the whole pump-laser chain. But this time with precautions taken to reduce air turbulences: the flowboxes are turned off, the stretcher box is sealed more carefully and beam tubes are installed inside the compressor. This measurement can be directly compared to Fig. 3(a) and shows a significantly improved timing jitter. The reduced jitter enables us to see two separate components to the remaining timing jitter: a shot-to-shot variation of ± 70 fs superimposed on a slow temporal drift of ± 200 fs.

An active stabilization system can easily correct for this large amplitude, slow fluctuation. In our active stabilization scheme we take the centroid wavelength of the SFG spectra on every shot, calculate the difference to a reference wavelength and move a delay stage (in the pump-chain cf. Fig. 1) to return to the reference position in cases, when the difference exceeds a certain value. This threshold is a parameter to optimize the active stabilization. If the threshold is too close to the shot to shot noise level, the delay stage will move on nearly every shot and the stabilization will become unstable. In the experiment, it was shown that the stabilization currently works best with this limit set to 100 fs. In this case we can stabilize the jitter to 105 fs Std, as shown in Fig. 3(d). This is sufficiently low for carrying out the first OPCPA experiments.

5. Theoretical considerations for optical path length inside a stretcher/compressor

The experiments indicated that the optical delay inside the stretcher-compressor setup is fraught with a much larger timing jitter compared to the same optical delay inside the regenerative amplifier. Furthermore it was shown that reducing the air turbulence resulted in a significant decrease of the timing jitter. In this section we will discuss the effect of turbulent air flow on the optical path length differences theoretically. The main feature of turbulent air is an inhomogeneous density which causes local refractive index gradients. A passing light beam will be refracted on such a refractive index step and is slightly deflected. For example a simulation for dry air at constant pressure shows, that a temperature change of 0.1K at room temperature can cause deflections in the range of μrad , if grazing incidence is considered. As many of these inhomogeneities are distributed randomly over the entire path length, we model the effect of turbulent air by assuming a mean angular deviation occurring at a mean position throughout the following analysis

At first let us consider a free-space propagation with the speed of light c over the distance x and a distance x_1 with a small angle difference $\Delta\alpha$ (compare Fig. 4). The timing difference can be calculated as

$$\Delta\tau = \frac{x_1 - x}{c} = \frac{x}{c} \left(\frac{1}{\cos(\Delta\alpha)} - 1 \right) \approx \frac{x \cdot \Delta\alpha^2}{2c} \quad (1)$$

For relatively large values $x = 100$ m and $\Delta\alpha = 10 \mu\text{rad}$ one obtains $\Delta\tau = 0.017$ fs and can therefore neglect this timing change for probably all experimentally relevant cases in the laboratory.

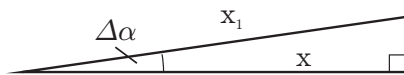


Fig. 4. Schematic picture for calculating the timing difference of light traveling along the paths x and x_1 .

In the following we will discuss the influence of beam pointing fluctuations on the optical path length inside a compressor. We derive the analytical expression for the path length difference as a function of the angle deviation $\Delta\beta$ and the location of this angle change d for the general case, with a few μrad angle deviation originating inside the compressor. Additionally, the special case of beam pointing of few μrad at the compressor input is discussed.

In most systems, the compressor is located in vacuum in order to avoid nonlinearities in air (our compressor is not vacuum sealed, yet). Therefore, the stretcher will be the most likely source of perturbations by air fluctuations. Nevertheless, we will analyze a compressor because the optical path is more easy to explain. These considerations are also valid for the stretcher setup, as the stretcher provides the same amount of dispersion but with opposite sign. However, the additional imaging system increases the optical path compared to the compressor, making the stretcher even more sensitive to air turbulence.

In the following we investigate the influence of a perturbation of the angle inside the compressor. Fig. 5 shows a double-grating double-pass Treacy compressor setup with a grating separation L_1 , aligned for an angle of incidence (AOI) α . The optical path of a ray with wavelength λ_0 and AOI of α is shown in red. The diffraction from the first grating is given by the grating equation

$$\beta = \arcsin(mN\lambda_0 - \sin\alpha). \quad (2)$$

where N is the line density, λ_0 is the center wavelength and m is the diffraction order. As the AOI on the second grating is β the beam diffracts at an angle α and impinges perpendicular on the end mirror from where it takes the same path back through the compressor.

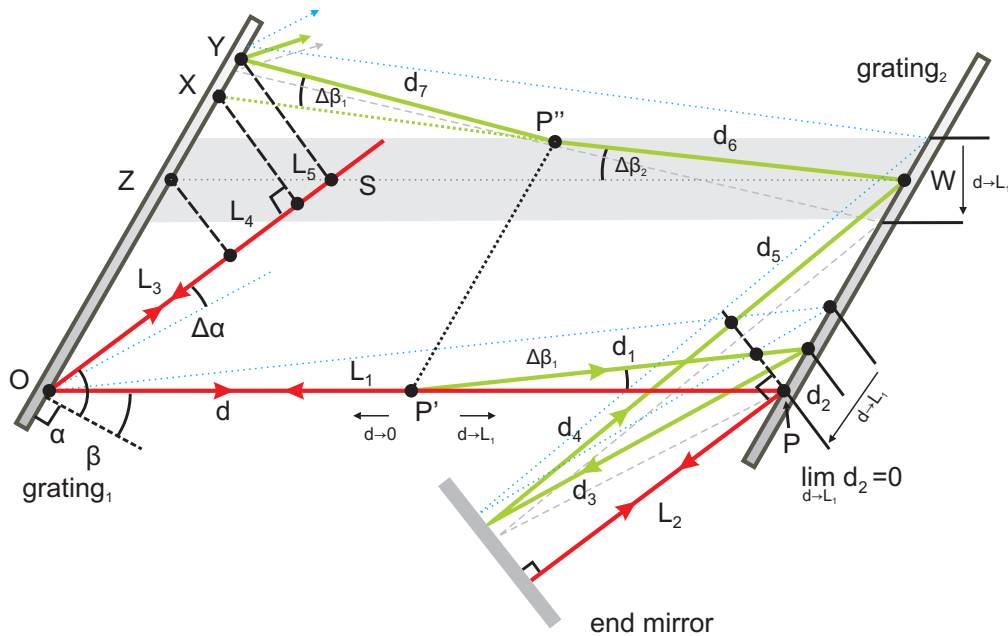


Fig. 5. Ray diagram illustrating the change in the optical path inside the grating compressor for the center wavelength λ_0 . The red ray shows the undisturbed case with an AOI of α . The green curve depicts the beam path of the pulse for the case when it is distorted at an angle $\beta + \Delta\beta_1$ at a distance d from the first grating. The blue, dotted and the gray, dashed traces show the extreme cases $d = 0$ and $d = L_1$, respectively. The case $d = 0$ corresponds to a different AOI of $\alpha - \Delta\alpha$ at the compressor input. For detailed explanation see main text.

A shot-to-shot pointing fluctuation inside the dispersion plane of the compressor can be described as a deviation $\Delta\beta_1$ from the design angle β which leads to a non-zero AOI on the end mirror of $\Delta\alpha$. This in turn results in a different path (and angle) for the first pass ($\beta + \Delta\beta_1$) and the return pass through the compressor ($\beta - \Delta\beta_2$), as shown in Fig. 5 (green). The location where the angle change takes place is parametrized with the parameter d . The extreme case $d = 0$ represents beam pointing at the compressor input O (or pointing with $\Delta\alpha$ outside the compressor), and $d = L_1$ stands for fluctuations at the position of the second grating. The angle change represents air fluctuations, which can be considered static on the time scale of a propagating light pulse. In Fig. 5 the angle deviations are magnified to better distinguish the different paths. In reality the points P' and P'' are closely adjacent. Therefore the same deviation as on point P' is present on the way back through the system at point P'' . (In the case when $d = 0$, P'' is on the first grating and would result in a small angle change of the outgoing beam. This effect is not relevant for the timing and is therefore neglected.)

The optical path lengths between point O and plane YS for the aligned and the slightly perturbed case are given by

$$p(\beta) = L_1 + L_2 + L_2 + L_1 + L_3 + L_4 + L_5, \text{ and} \quad (3)$$

$$p(\beta + \Delta\beta_1) = d + d_1 + d_2 + d_3 + d_4 + d_5 + d_6 + d_7, \text{ respectively.} \quad (4)$$

The timing difference can then be calculated by $\Delta\tau = (p(\beta) - p(\beta + \Delta\beta_1))/c$. The paths L_1 and L_2 are given by the compressor design, d is a parameter and the other path lengths can be obtained from general trigonometric relations in Fig. 5:

$$d_1 = (L_1 - d) \frac{\cos\beta}{\cos(\beta + \Delta\beta_1)} \quad (5)$$

$$d_2 = (L_1 - d) \frac{\sin(\Delta\beta_1)}{\cos(\beta + \Delta\beta_1)} \frac{\sin\alpha}{\cos(\Delta\alpha)} \quad (6)$$

$$d_3 = d_4 = \frac{L_2}{\cos(\Delta\alpha)} \quad (7)$$

$$d_5 = (d_2 + d_3) \frac{\cos(\alpha - \Delta\alpha)}{\cos(\alpha + \Delta\alpha)} - d_4 \quad (8)$$

$$d_6 = (L_1 - d) \frac{\cos\beta}{\cos(\beta - \Delta\beta_2)} \quad (9)$$

$$d_7 = d \frac{\cos\beta}{\cos(\beta - \Delta\beta_1 - \Delta\beta_2)} \quad (10)$$

$$L_3 = d_5 \cos(\Delta\alpha) \quad (11)$$

$$L_4 = L_1 \frac{\sin(\Delta\beta_2)}{\cos(\beta - \Delta\beta_2)} \sin\alpha \quad (12)$$

$$L_5 = d \frac{\cos\beta}{\cos(\beta - \Delta\beta_2)} \cdot \frac{\sin(\Delta\beta_1)}{\cos(\beta - \Delta\beta_1 - \Delta\beta_2)} \sin\alpha \quad (13)$$

The contribution to the timing difference from $2L_2 - d_3 - d_4$ has the same form as in the free space case, discussed above (Eq. (1)), and can therefore be neglected. In this approximation, the timing difference is independent of the distance of the end mirror to the second grating L_2 . For the same reason $L_3 - d_5$, which accounts for a parallel offset of plane \overline{OP} and \overline{WZ} , has a

negligible effect on the timing difference. The total timing difference can then be written:

$$\begin{aligned}
\Delta\tau &= \frac{1}{c}(2L_1 - d - d_1 - d_6 + L_4 - d_2 + L_5 - d_7) \quad (14) \\
&= \frac{L_1}{c} \left(2 - \frac{\cos\beta + \sin(\Delta\beta_1)\sin\alpha}{\cos(\beta + \Delta\beta_1)} - \frac{\cos\beta - \sin(\Delta\beta_2)\sin\alpha}{\cos(\beta - \Delta\beta_2)} \right) \\
&+ \frac{d}{c} \left(\frac{\cos\beta + \sin(\Delta\beta_1)\sin\alpha}{\cos(\beta + \Delta\beta_1)} - 1 \right) \\
&+ \frac{d}{c} \left(\frac{\cos\beta}{\cos(\beta - \Delta\beta_2)} \left[1 - \frac{\cos(\beta - \Delta\beta_2) - \sin(\Delta\beta_1)\sin\alpha}{\cos(\beta - \Delta\beta_1 - \Delta\beta_2)} \right] \right) \quad (15)
\end{aligned}$$

With the help of the grating equation (Eq. (2)) we can write $\sin\alpha$ in terms of $\sin\beta$. For small angles $\Delta\beta$ we can approximate $\sin(\Delta\beta) \approx \Delta\beta$ and $\cos(\Delta\beta) \approx 1$. Under this approximation it follows that $\cos(\beta \pm \Delta\beta) \approx \cos\beta \mp \Delta\beta \sin\beta$. Equation (15) can then be approximated as

$$\begin{aligned}
\Delta\tau &\approx \frac{L_1 m N \lambda_0}{c} \left(\frac{\Delta\beta_2}{\cos(\beta - \Delta\beta_2)} - \frac{\Delta\beta_1}{\cos(\beta + \Delta\beta_1)} \right) \\
&+ \frac{d m N \lambda_0}{c} \left(\frac{\Delta\beta_1}{\cos(\beta + \Delta\beta_1)} \right) \\
&+ \frac{d m N \lambda_0}{c} \frac{\cos\beta}{\cos(\beta - \Delta\beta_2)} \left(\frac{\Delta\beta_1}{\cos(\beta - \Delta\beta_1 - \Delta\beta_2)} \right). \quad (16)
\end{aligned}$$

The following calculations are done for the approximated expression (Eq. (16)) as well as for the formula without approximations (Eq. (15)) with the following parameters: $N = 1740$ lines/mm, $\lambda_0 = 1030$ nm, $m = 1$, $L_1 = 6$ m, $L_2 = 3$ m and $\alpha = 58.5^\circ$, as in the experimental setup. It should be noted, that we are interested in small angle changes (few μ rad) which may affect the optical path length, but do not change the pulse length or angular chirp [18] in a significant way.

In these formulae it can be seen, that smaller angles β are favorable in terms of timing difference. Nevertheless, in order to compare the jitter for different angles one has to take into account that the dispersion is also decreasing with decreasing β . Therefore the compressor length should be adapted to compare compressors with the same dispersion. For example our compressor is designed in a reverse configuration where $\alpha < \beta$ ($\alpha = 58.5^\circ$, $\beta = 69.98^\circ$) because in this case the necessary dispersion can be achieved with only $L_1 = 6$ m grating separation. Another option would be the normal configuration with $\alpha = 69.98^\circ$, $\beta = 58.5^\circ$ where a grating separation of $L_1 = 14$ m is needed. This configuration is also considered in the following paragraphs.

5.1. Angle fluctuations at the compressor input

The special case $d = 0$ corresponds to the situation, when there is a certain beam pointing fluctuation $\Delta\alpha$ at the compressor input. This change translates to a fluctuation $\Delta\beta_1$ to the diffracted beam at point O on the first grating. No source of angle fluctuation inside the compressor is considered. For $d = 0$, the last two terms in Eq. (15) and Eq. (16) vanish and Eq. (16) takes the form

$$\begin{aligned}
\Delta\tau &= \frac{1}{c}(2L_1 - d_1 - d_6 + L_4 - d_2) \quad (17) \\
&= \frac{L_1 m N \lambda_0}{c} \left(\frac{\Delta\beta_2}{\cos(\beta - \Delta\beta_2)} - \frac{\Delta\beta_1}{\cos(\beta + \Delta\beta_1)} \right) \quad (18)
\end{aligned}$$

The effect of angular deviation outside the compressor on the timing is very small because d_1 is a bit longer than L_1 but d_6 is a bit shorter and together they nearly cancel out each other,

i.e. $d_1 + d_6 \approx 2L_1$. Additionally d_2 and L_4 compensate each other, i.e. $d_2 \approx L_4$ (compare Fig. 5, Eqs. (5)–(13)). From Eq. (18) it can be seen that the remaining difference occurs because $\Delta\beta_1 \neq \Delta\beta_2$. This is due to the fact, that the angle $\beta + \Delta\beta$ is transferred to $\beta - \Delta\beta$ after reflection off the end mirror. Thus the effect of angular deviation taking place outside the compressor on the timing is very small.

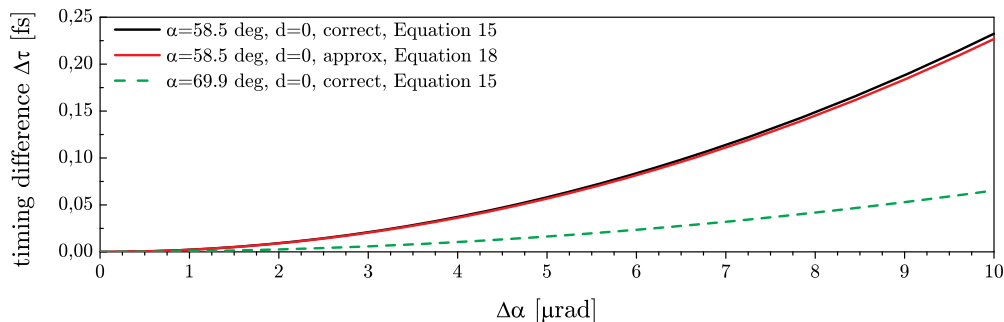


Fig. 6. Timing difference for a small change $\Delta\alpha$ of the AOI α at the compressor input ($d=0$). Larger angle α (smaller angle β) is advantageous in terms of jitter.

In Fig. 6 the calculated timing jitter due to pointing fluctuations at the compressor input is shown. For pointing fluctuations up to $10 \mu\text{rad}$ the timing jitter is less than 0.25 fs, which was also checked via ray tracing. We measured the beam pointing at the compressor input to be less than $1 \mu\text{rad}$ which corresponds to 0.0025 fs jitter. This jitter is negligible in our case. Nevertheless, it should be noted that this timing jitter from angular deviations outside the compressor is two orders of magnitude larger than the effect of the same angle deviation in a freely propagating beam over the same distance (compare Eq. (1)) and that the compressor configuration with $\alpha > \beta$ would have advantages in terms of jitter, even though the grating separation is more than doubled to achieve the same dispersion.

5.2. Angle fluctuations inside the grating compressor

In the previous paragraph we have shown, that angle fluctuations at the compressor input are negligible because all path lengths compensate each other to a large extent. So we will have a look at the influence of angle fluctuations originating inside the compressor. From Fig. 5 one can understand what happens when d is increased, the distances on the way to the end mirror (d_1, d_2) are decreasing and can not compensate for the distances during the back propagation (d_7, L_4, L_5) and the timing difference is drastically increased.

In Eqs. (15) and (16) we can neglect the first term as shown in the previous paragraph. It turns out, that the second and the third term in Eq. (16) both have the same weight. When approximating $\cos(\beta + \Delta\beta) \approx \cos\beta$ we can further simplify Eq. (16) to:

$$\Delta\tau \approx \frac{2mN\lambda_0}{c \cos\beta} \Delta\beta_1 \cdot d \quad (19)$$

Figure 7(a) shows that the approximations for Eq. (19) are well justified, because deviations from the non-approximated curve are negligible. As predicted by Eq. (19), the linear character in d and $\Delta\beta$ shows clearly in the graphs. Compared to the case with $d = 0$ the jitter is up to 4 orders of magnitude higher (for $d = L_1$) and again the normal configuration with smaller β (larger α) has advantages in terms of sensitivity to timing jitter. Figure 7(b) shows the timing jitter for different positions d . As mentioned earlier the effect of turbulent air is modeled by assuming

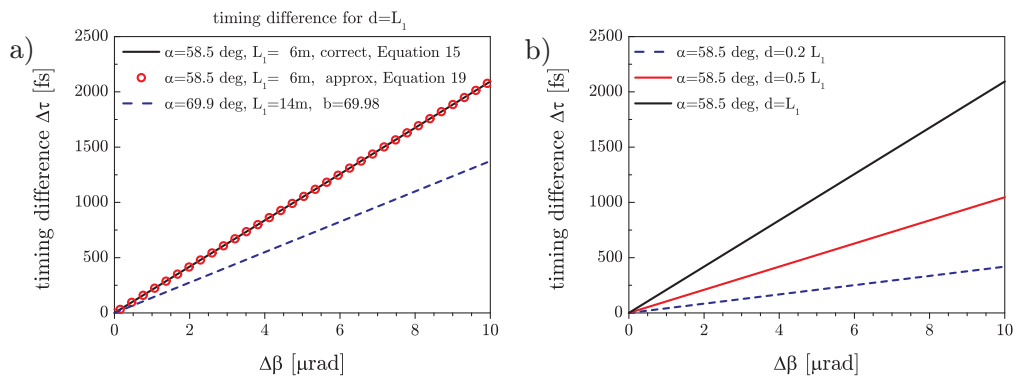


Fig. 7. a) Timing difference for $d = L_1$: the approximations in Eq. (19) are well justified in the considered range. The configuration with increased AOI α (or decreased β) shows reduced timing differences. b) Timing difference for different values of d .

a mean angular deviation at a mean position. Since the mean position is most likely located at $d = 0.5 L_1$, the corresponding curve is most suitable to reflect the effect of air turbulence.

As a result of this analysis we can state that a Treacy-type compressor introduces a timing jitter, when a beam pointing is considered. Beam pointing fluctuations at the compressor input are orders of magnitude less critical than those occurring inside the compressor, especially close to the second grating. With this calculation we can explain the effect of beam pointing fluctuations, as could be introduced by air turbulence or mechanical instabilities of optical elements like gratings, mirror or imaging optics (in case of a stretcher). Generally a smaller angle β is preferable in terms of jitter even if a longer path is needed to get the necessary dispersion.

6. Summary

In conclusion, we have quantitatively investigated the level of timing synchronization between the pump and seed pulses of the PFS system, which is currently under development. Additionally an active stabilization system is applied which eliminates the slow drift and reduces the jitter to 100 fs Std. This will enable the first short-pulse pumped OPCPA experiments with our system.

Using the spectral gating technique we succeeded in demonstrating experimentally that the air fluctuations inside the stretcher-compressor setup are the main source of the pump-seed timing jitter. In addition we have provided a theory on timing difference due to angular deviations inside a stretcher/compressor. As the main result the beam pointing fluctuation at the stretcher/compressor input accounts only for less than 0.2 fs jitter whereas angle fluctuations of the same magnitude originating inside the stretcher/compressor can result in up to four orders of magnitude larger jitter, depending on where this perturbation is located inside the compressor. This theory provides a simple formula (Eq. (19)) and can perfectly explain the experimental observations. Although the grating stretcher and compressor were extensively investigated in the past (e.g. [14, 16, 18, 19]), to the best of our knowledge a sensitivity of these components for absolute timing jitter has not been reported up to now. Most probably because timing sensitive applications such as our CPA pumped ps OPCPA have been emerging in the past few years (c.f.: [12, 20, 21]). All these systems are quite different, but have one thing in common: An increased timing jitter after compression at the final stage is measured, compared to an early stage of the setup. With the presented theory it is now possible to explain a major part of the

observed increase in the timing jitter.

Air fluctuations inside a compressor are not relevant in most CPA systems, since usually compressors are situated in vacuum in order to avoid nonlinearities in air. Nevertheless the calculations are also valid for the stretcher. Therefore any air fluctuations or vibrations inside the stretcher should be avoided, if low temporal jitter is required. This means, ideally the stretcher would also be in a vacuum environment for such cases.

As a consequence of our findings we plan to enclose the stretcher in an air-tight container. If this proves to be insufficient in the future, we might even go to vacuum. For the compressor a large vacuum tank will be constructed (ca. $4.5 \times 1.5 \times 1 \text{ m}^3$), in contrast to the original plan, where only the last grating should be placed in a considerably smaller chamber. These improvements will help in eliminating the air fluctuations and hence the large timing instabilities altogether.

Acknowledgments

This work was funded by the Max-Planck Society through the PFS grant. Financial support from the Extreme Light Infrastructure and the DFG Cluster of Excellence, Munich Centre for Advanced Photonics, is also acknowledged.